

## Specific Targeting of Tumor Endothelial Cells by a Shiga-like Toxin–Vascular Endothelial Growth Factor Fusion Protein as a Novel Treatment Strategy for Pancreatic Cancer<sup>1</sup>

Birgit Hotz<sup>\*</sup>, Marina V. Backer<sup>†</sup>, Joseph M. Backer<sup>†</sup>, Heinz-J. Buhr<sup>\*</sup> and Hubert G. Hotz<sup>\*</sup>

<sup>\*</sup>Department of Surgery I, Charité School of Medicine, Campus Benjamin Franklin, Berlin, Germany; <sup>†</sup>SibTech, Inc, Brookfield, CT, USA

### Abstract

**PURPOSE:** Tumor endothelial cells express vascular endothelial growth factor receptor 2 (VEGFR-2). VEGF can direct toxins to tumor vessels through VEGFR-2 for antiangiogenic therapy. This study aimed to selectively damage the VEGFR-2–overexpressing vasculature of pancreatic cancer by SLT–VEGF fusion protein comprising VEGF and the A subunit of Shiga-like toxin which inhibits protein synthesis of cells with high VEGFR-2 expression. **EXPERIMENTAL DESIGN:** Expression of VEGF and VEGF receptors was evaluated in human pancreatic cancer cells (AsPC-1, HPAF-2) and in normal human endothelial cells (HUVEC) by reverse transcription–polymerase chain reaction. Cells were treated with SLT–VEGF (0.1–10 nM), and cell viability, proliferation, and endothelial tube formation were assessed. Orthotopic pancreatic cancer (AsPC-1, HPAF-2) was induced in nude mice. Animals were treated with SLT–VEGF fusion protein alone or in combination with gemcitabine. Treatment began 3 days or 6 weeks after tumor induction. Primary tumor volume and dissemination were determined after 14 weeks. Microvessel density and expression of VEGF and VEGF receptors were analyzed by immunohistochemistry. **RESULTS:** SLT–VEGF did not influence proliferation of pancreatic cancer cells; HUVECs (low-level VEGFR-2) reduced their proliferation rate and tube formation but not their viability. SLT–VEGF fusion protein reduced tumor growth and dissemination, increasing 14-week survival (AsPC-1, up to 75%; HPAF-2, up to 83%). Results of gemcitabine were comparable with SLT–VEGF monotherapy. Combination partly increased the therapeutic effects in comparison to the respective monotherapies. Microvessel density was reduced in all groups. Intratumoral VEGFR-2 expression was found in endothelial but not in tumor cells. **CONCLUSIONS:** SLT–VEGF is toxic for tumor vasculature rather than for normal endothelial or pancreatic cancer cells. SLT–VEGF treatment in combination with gemcitabine may provide a novel approach for pancreatic cancer.

*Neoplasia* (2010) 12, 797–806

### Introduction

Adenocarcinoma of the exocrine pancreas is the fifth leading cause of cancer-related death in Western countries. The estimated overall 5-year survival rate of less than 5% is due to the tumor's propensity toward aggressive growth, early metastasis, and resistance to cytotoxic agents and radiation. More than 80% of patients are diagnosed with pancreatic cancer at a locally advanced or metastatic stage, which excludes a curative surgical resection [1]. New therapeutic approaches based on the biologic characteristics of this disease may improve response rates and survival. One promising approach is the inhibition of angiogenesis. Like all solid neoplasms, pancreatic cancer depends on the process of angiogenesis, the formation of tumor blood vessels, for both local and metastatic

growth beyond the size of a few cubic millimeters [2]. Inhibition of angiogenesis is an attractive target for tumor therapy because it theoretically offers the hope of long-term control of neoplasm progression [3]. Among the identified proangiogenic regulators, vascular endothelial

Address all correspondence to: Hubert G. Hotz, MD, Department of Surgery I, Charité School of Medicine, Campus Benjamin Franklin, Hindenburgdamm 30, 12203 Berlin, Germany. E-mail: [hubert.hotz@charite.de](mailto:hubert.hotz@charite.de)

<sup>1</sup>This article refers to supplementary materials, which are designated by Figures W1 and W2 and are available online at [www.neoplasia.com](http://www.neoplasia.com).

Received 17 March 2010; Revised 16 June 2010; Accepted 22 June 2010

Copyright © 2010 Neoplasia Press, Inc. All rights reserved 1522-8002/10/\$25.00  
DOI 10.1593/neo.10418

growth factor (VEGF; a.k.a. VEGF-A) and its two tyrosine kinase receptors, the *fms*-like tyrosine kinase receptor (Flt1, VEGFR-1) and the kinase insert domain-containing receptor (KDR/FLK1, VEGFR-2), have been identified as key mediators of the regulation of pathologic blood vessel growth and maintenance [4]. VEGF induces endothelial cell proliferation and enhances vascular permeability [5]. Previous studies have shown that VEGF is overexpressed in human pancreatic cancer [6–8]. Moreover, a high expression of VEGF was associated with liver metastasis and a poor prognosis for patients with ductal pancreatic adenocarcinoma [9,10]. In most epithelial tumors, including pancreatic cancer, VEGFR-1 and VEGFR-2 are expressed almost exclusively on endothelial cells, and there is evidence that endothelial cells at sites of angiogenesis express significantly higher numbers of VEGFR-2—the key proangiogenic receptor—than quiescent endothelial cells [11]. Blocking the effects of VEGF on endothelial cells by receptor antagonists [12–14] or neutralizing anti-VEGF antibodies [15,16] inhibits the expansion of a variety of neoplasms. However, there is recent evidence that the effects of these anti-VEGF strategies seem to be transient, in particular when the treatment is interrupted [17].

An alternative approach to destroy tumor endothelium would be a targeted delivery of potent toxins to tumor endothelial cells. We conducted *in vitro* and *in vivo* experiments to evaluate the effects of SLT-VEGF fusion protein comprising VEGF<sub>121</sub> and catalytically active A subunit of Shiga-like toxin 1 (SLT-1) produced by *Escherichia coli* O157:H7 [18,19]. SLT-1 is composed of a single copy of a 32-kDa A subunit associated with a ring-shaped pentamer of 7-kDa B subunits that bind to the cellular receptor globotriaosylceramide known as Gb3/CD77 and enters cells through CD77-mediated endocytosis. SLT-1 was chosen as a potential “natural killer” of endothelial cells because it is known that damage to endothelial cells caused by SLT-1 plays a causative role in the pathogenesis of hemorrhagic colitis and hemolytic uremic syndrome induced by *E. coli* O157:H7 [20,21]. SLT-VEGF is internalized through VEGFR-2 mediated endocytosis, and its cytotoxicity correlates with VEGFR-2 expression [18]. In animal tumor models, SLT-VEGF selectively depletes VEGFR-2-overexpressing CD31<sup>+</sup> endothelial cells in tumor vasculature as judged by immunohistochemical analysis [19] and whole body imaging of VEGF receptors [22]. In contrast, CD31<sup>+</sup> tumor endothelial cells that express relatively low levels of VEGFR-2 are marginally affected by SLT-VEGF [19].

The aim of this study was to evaluate a novel antiangiogenic treatment strategy for pancreatic cancer by selectively damaging endothelial cells at sites of angiogenesis with SLT-VEGF in a clinically relevant orthotopic nude mouse model of pancreatic cancer. In addition, we investigated whether a combination of SLT-VEGF with the cytotoxic agent gemcitabine increases the therapeutic potential in this animal model. As a control, we assessed the effects of SLT-VEGF on proliferation and viability of the human pancreatic cancer cell lines AsPC-1 and HPAF-2 and the human endothelial cell line HUVEC *in vitro*.

## Materials and Methods

### Cell Line and Culture Conditions

The human pancreatic adenocarcinoma cell lines AsPC-1 (ATCC, CRL-1682) and HPAF-2 (ATCC, CRL-1997) of ductal origin and the noncancerous endothelial cell line HUVEC (C-12200) were obtained from the American Type Culture Collection (ATCC, Manassas, VA) and from PromoCell GmbH (Heidelberg, Germany). The cells were cultured in RPMI-1640 medium (AsPC-1; Invitrogen, Karlsruhe, Germany), minimum essential medium (HPAF-2; PAA, Cölbe, Ger-

many), or endothelial cell growth medium (HUVEC; PromoCell), supplemented with 10% heat-inactivated fetal bovine serum (FBS-Gold; PAA), penicillin G (100 U/ml), streptomycin (100 µg/ml), and amphotericin B (0.25 mg/ml). Cells were incubated at 37°C in humidified air with 5% CO<sub>2</sub>. The medium was replaced twice a week, and cells were maintained by serial passaging after treating with 0.1% trypsin.

### Reverse Transcription–Polymerase Chain Reaction

Total cellular RNA was extracted from cell cultures using the NucleoSpin RNA II Kit (Macherey & Nagel, Düren, Germany) according to the manufacturer's instructions and resuspended in 50 µl of water treated with 0.1% DMPC (Sigma-Aldrich, Seelze, Germany). RNA concentration was determined using a BioPhotometer (Eppendorf Scientific, Hamburg, Germany). Reverse transcription of total RNA (2 µg) primed with an oligo(dT) oligonucleotide and supplemented with dNTPs (Sigma-Aldrich) was done with M-MLV reverse transcriptase (Promega, Mannheim, Germany) according to the instructions of the manufacturer. First-strand complementary DNA was amplified with transcript-specific oligonucleotides using Ready-Mix Taq PCR Reaction Mix (Sigma-Aldrich).

The primers (TIB MOLBIOL, Berlin, Germany) for the respective genes were designed as follows: VEGF, sense 5'-CGA AGT GGT GAA GTT CAT G-3' and antisense 5'-TTC TGT ATC AGT CTT TCC TGG TGA G-3'; Flt1/VEGFR-1, sense 5'-GAA GGC ATG AGG ATG AGA GC-3' and antisense 5'-CAG GCT CAT GAA CTT GAA AGC-3'; KDR/FLK1/VEGFR-2, sense 5'-CAT GTA CGG TCT ATG CCA TTC-3' and antisense 5'-CGT TGG CGC ACT CTT CCT-3'; and β-actin, sense 5'-TTC CTG GGC ATG GAG TCC TGT GG-3' and antisense 5'-CGC CTA GAA GCA TTT GCG GTG G-3'.

Polymerase chain reaction (PCR) products and a 100-bp DNA molecular weight marker were analyzed by electrophoresis on a 1% agarose gel. The gel was then visualized and photographed under ultraviolet light.

### SLT-VEGF Fusion Protein

SLT-VEGF fusion protein was constructed, expressed in *E. coli* strain Origami(DE3)pLysS (Novagen, Madison, WI), purified, and extensively characterized *in vitro* and *in vivo* as described elsewhere [18,19,22]. SLT-VEGF retained physical integrity and functional activity after 2 hours of incubation in murine serum at 37°C (Supplementary Material and Figure W1). However, SLT-VEGF was inactivated by conjugation of a single fluorescent dye (Supplementary Material and Figure W2). For *in vitro* assays and intraperitoneal injection, SLT-VEGF was dissolved in 0.9% NaCl (pH 7.5). Further dilutions for *in vitro* studies were made with medium and filtered before use.

### In Vitro Assessment of Cell Proliferation and Viability

To examine the effect of SLT-VEGF on *in vitro* cell proliferation, 2 × 10<sup>5</sup> cells from the human pancreatic cancer cell lines AsPC-1, HPAF-2, and the noncancerous human endothelial cell line HUVEC were seeded in six-well culture plates in 2 ml of the respective cell culture medium. The medium was changed the next day (day 1) and SLT-VEGF (0.1–10 nM) was added. After 72 hours (day 4), the cells were trypsinized and counted in a standard hemocytometer. Cell viability was assessed by a colorimetric dye reduction assay with monotetrazolium (MTT; Boehringer, Mannheim, Germany) according to the manufacturer's instructions. Briefly, cells were seeded in 96-well plates at a density of 5 × 10<sup>3</sup> cells per well in 0.2 ml of the respective medium. Medium was changed the next day (day 1), and SLT-VEGF (0.1–10 nM) was added

to triplicate wells. After 72 hours (day 4), 10  $\mu$ l of MTT (5 mg/ml) solution, and after additional 4 hours of incubation at 37°C 10%, SDS was added to the cells, 100  $\mu$ l per well. The plates were allowed to stand overnight (37°C at 5% CO<sub>2</sub>). The change in absorbance measured at 550 nm with a plate reader (Biotek Instruments, Inc, Burlington, VT) has been shown to strongly correlate with the number of viable cells. All experiments were generated in triplicates and repeated three times.

### *In Vitro* Capillary Tube Formation Assay

The ability of SLT-VEGF fusion protein to inhibit angiogenesis *in vitro* was evaluated in a capillary tube formation assay using HUVECs cultured on a synthetic basement membrane matrix. Under these conditions, HUVECs are capable of morphologic differentiation into an extensive network of capillary-like structures composed of highly organized three-dimensional cords [23]. The 96-well cell culture plates were coated with a 100- $\mu$ l layer of the synthetic basement membrane substrate Matrigel (Becton Dickinson, Heidelberg, Germany) at 10 mg/ml concentration and were incubated at 37°C for 30 minutes to promote gelling. HUVECs were seeded in coated plates,  $1.8 \times 10^4$  cells per well, SLT-VEGF fusion protein was diluted in cell medium and added to HUVECs in triplicate wells to final concentrations of 1 or 10 nM. Stimulation with VEGF (250 pg/ml) served as positive control. After an 18-hour incubation at 37°C and 5% CO<sub>2</sub> humidified atmosphere, the complete capillary tube network within a designated area of a low magnification ( $\times 10$ ) field was counted under light microscopy, and data were expressed as percentage of complete capillary tube formation relative to untreated HUVEC control cultures incubated under the same conditions. The assays were done in triplicates in three independent experiments.

### Orthotopic Nude Mouse Model of Pancreatic Cancer

We used the transplantation technique previously described for an orthotopic nude mouse and rat model of pancreatic cancer [24,25]. Four-week-old male nude mice were obtained from Charles River Laboratories (Charles River, Sulzfeld, Germany). Donor mice were anesthetized with isoflurane (Forene; Abbott, Wiesbaden, Germany) inhalation. Ten million cells of either the AsPC-1 or HPAF-2 cell line were injected subcutaneously into the animals' flanks. The animals were killed by a lethal dose of isoflurane inhalation and opening of the thorax after 4 weeks, when the subcutaneous tumors had reached a size of 1 cm in largest diameter. The donor tumors were harvested and minced by a scalpel (no. 11) into small (1 mm<sup>3</sup>) fragments. Tumor recipient nude mice were anesthetized with isoflurane, followed by intraperitoneal injection of xylazine hydrochloride (Rompun, 12 mg/kg body weight [BW]; Bayer, Leverkusen, Germany) and Esketaminhydrochloride (Ketanest S, 40 mg/kg BW; Parke-Davis/Pfizer, Karlsruhe, Germany). The animals' abdomens were opened by a midline incision, and the pancreatic tail with the spleen was gently exteriorized. Two small tissue pockets were prepared in the pancreatic parenchyma as an implantation bed with a microscissor (RS-5610 VANNAS; Roboz, Rockville, MD). One donor tumor fragment was placed into each pancreatic tissue pocket in such a way that the neoplastic tissue was completely surrounded by pancreatic parenchyma. The pancreas was relocated into the abdominal cavity, which was then closed in two layers with 4-0 absorbable suture (Vicryl, Ethicon, Germany). For pain relief, a subcutaneous injection of carprofen (Rimadyl, 4 mg/kg BW; Pfizer) was given after surgery.

### *In Vivo* Treatment with SLT-VEGF and Gemcitabine

The animals were allocated randomly into four treatment groups (SLT-VEGF, prophylaxis and therapy; SLT-VEGF and gemcitabine, prophylaxis and therapy) and one control group. Administration of SLT-VEGF (200  $\mu$ g/kg, intraperitoneally every second day), of gemcitabine (125 mg/kg, intraperitoneally once a week), as well as the combination of both substances began either 3 days (prophylaxis) or 6 weeks (therapy) after tumor induction. Control animals received equivalent amounts of saline. The therapy was continued up to 14 weeks after tumor induction.

### Quantification of Tumor Growth and Spread

All animals underwent autopsy after 14 weeks after the orthotopic tumor implantation by a lethal dose of isoflurane. The perpendicular diameters of the primary orthotopic tumor were measured with calipers, and the volume was calculated using the following formula: volume = length  $\times$  width  $\times$  depth / 2. A dissemination score was used to assess local tumor infiltration as well as distant metastasis [24,25]. Local infiltration was determined at the following sites: spleen, stomach, liver (hilus), kidney, retroperitoneum, diaphragm, mesentery, bowel loops, and abdominal wall. Isolated tumor nodules with no anatomic connection to the primary tumor were considered distant metastases. The sites of evaluation included liver, kidney, spleen, lung, diaphragm, mesentery, retroperitoneum, mediastinum, and the suture line. Tumor dissemination was quantified as follows. Each manifestation of tumor infiltration or metastasis was credited with one point. Additional points were awarded for massive local infiltration (e.g., including more than half of the circumference of the spleen), multiple metastatic nodules ( $>1$  in parenchymal organs;  $>10$  in diaphragm, mesentery, and retroperitoneum), and metastatic nodules more than 50 mm<sup>3</sup>. Clinical consequences of tumor growth were incorporated into the following scoring system: formation of ascites (2 points if volume  $> 5$  ml), development of jaundice, ileus, and cachexia. The primary tumor and all sites of potential infiltration or metastasis were harvested, fixed in 4% formaldehyde, and embedded in paraffin. Then 3- $\mu$ m-thick tissue sections were obtained and stained with hematoxylin and eosin for microscopic examination. The sections were reviewed to confirm the findings of the macroscopic dissemination score.

### Immunohistochemistry

Immunohistochemical staining was performed on paraffin-embedded tissue of the collected primary tumor tissue. Three-micrometer-thick sections were cut, using a rotation microtome (RM2125RT; Leica, Wetzlar, Germany). The sections were deparaffinized in xylene and rehydrated in graded alcohols and distilled water. After antigen retrieval with 0.01% EDTA pH 8.0, endogenous peroxidase activity was blocked with 1% hydrogen peroxide in distilled water for 25 minutes followed by washing with distilled water and finally PBS + 0.1% Tween for 5 minutes. To bind nonspecific antigens, the sections were incubated with 1  $\times$  Power Block (BioGenex, San Ramon, CA) for 5 minutes. The primary antibodies were purified antirabbit CD-31 (platelet endothelial cell adhesion molecule), VEGF, VEGFR-1, and VEGFR-2 purchased from Santa Cruz Biotechnology (Santa Cruz, CA). Antibodies diluted 1:100 to 1:150 in antibody diluent (DCS LabLine, Hamburg, Germany) were applied to tissue sections and incubated for 30 minutes at 37°C. As a negative control, sections were incubated with antibody diluent instead of the primary antibody. This was followed by incubation with biotinylated antirabbit immunoglobulin G (1:200; Santa Cruz Biotechnology) for 30 minutes at 37°C. After washing with

PBS + Tween-20 and incubating with peroxidase-conjugated avidin-biotin complexes (KPL, Gaithersburg, MD), the immune complexes were visualized by 3,3'-diaminobenzidine (Sigma-Aldrich). The sections were then counterstained with Mayer hematoxylin, upgraded alcohols, mounted, and analyzed by standard light microscopy.

### Microvessel Density

Anti-CD31 was used as an endothelial marker to highlight intratumoral microvessels. Microvessel density (MVD) was quantified as described by Weidner [26]. Areas of highest neovascularization were found by scanning the sections at a magnification of  $\times 100$ , and individual microvessel counts were made on 10 fields at  $\times 200$  magnification ( $\approx 0.74 \text{ mm}^2$  per field).

### Statistical Analysis

All results are presented as mean  $\pm$  SEM. Continuous normally distributed variables were analyzed by the Student's *t* test. Discontinuous variables (dissemination score and MVD) were analyzed by the Mann-Whitney rank sum test. Differences in survival were tested by the  $\chi^2$  test.  $P < .05$  was considered as statistically significant.

## Results

### In Vitro

**Messenger RNA expression of VEGF and its receptors in human pancreatic cancer cell lines.** Expression of VEGF, Flt1/VEGFR-1 and KDR/FLK1/VEGFR-2 messenger RNA (mRNA) in the human pancreatic cancer cell lines AsPC-1 and HPAF-2 as well as in the human endothelial cell line HUVEC were determined with reverse transcription (RT)-PCR (Figure 1). All three cell lines exhibited both VEGF (400 bp) and Flt1/VEGFR-1 (300 bp) transcripts. Only HUVECs were positive for KDR/FLK1/VEGFR-2 (200 bp).

**Effect of SLT-VEGF on proliferation and cell viability.** The effect of SLT-VEGF on the proliferation and viability of the human pancreatic cell lines AsPC-1, HPAF-2, and the noncancerous human endothelial cell line HUVEC was studied during a period of 72 hours. HUVECs express relatively low numbers of VEGFR-2/cell ( $\sim 10$ -25,000) and therefore were not expected to be particularly sensitive to toxin-VEGF fusion proteins, as its cytotoxicity of such proteins

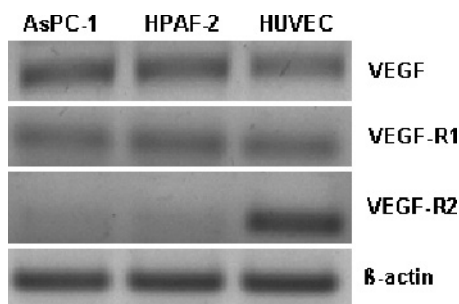


**Figure 1.** Expression of VEGF and its receptors Flt/VEGFR-1 and KDR/FLK1/VEGFR-2 in human pancreatic cancer cell lines (AsPC-1 and HPAF-2) and HUVEC endothelial cells measured by RT-PCR. VEGF and Flt/VEGFR-1 mRNA was detectable in all three cell lines, but KDR/FLK1/VEGFR-2 mRNA was only present in the endothelial cell line HUVEC.

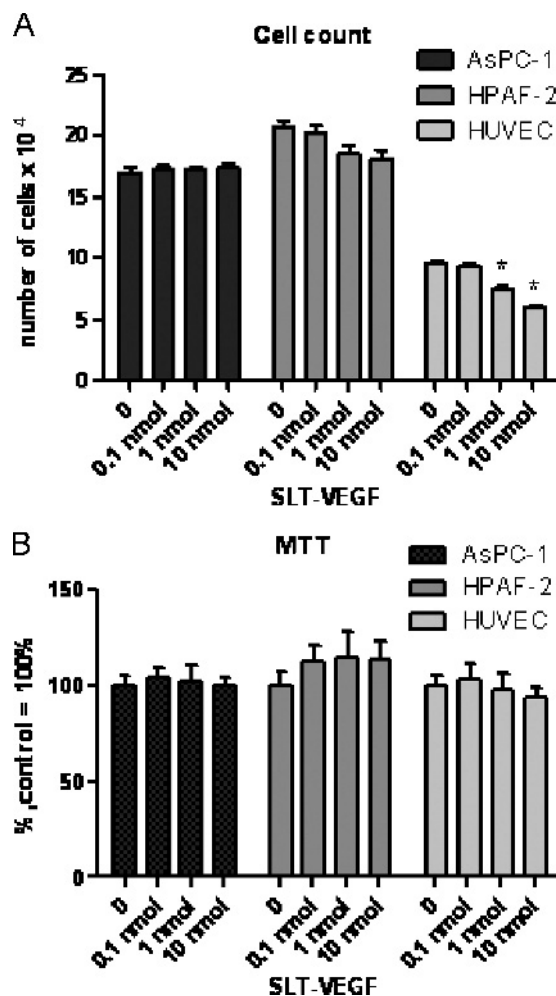


**Figure 2.** (A) *In vitro* effects of SLT-VEGF on proliferation of AsPC-1, HPAF-2, and HUVECs as assessed by cell count after 72 hours of incubation. Increased concentrations of SLT-VEGF inhibited proliferation of the human endothelial cell line HUVEC ( $*P < .001$ ). Proliferation of the pancreatic cancer cell lines AsPC-1 and HPAF-2 was not affected. (B) *In vitro* effects of SLT-VEGF on viability of AsPC-1, HPAF-2, and HUVECs as assessed by MTT assay after 72 hours of incubation. Even at high concentrations of SLT-VEGF (10 nM), viability of pancreatic cancer cells and endothelial cells was consistent.

strongly depends on the VEGFR-2 density in targeted cells [18,27]. The fusion protein was applied to the cells at three different final concentrations: 0.1, 1, and 10 nM. Figure 2 shows proliferation and viability changes during the treatment. Cell count and an MTT-assay indicate that SLT-VEGF did not influence proliferation of pancreatic cancer cells significantly, even at the highest concentrations (10 nM). Proliferation of the human endothelial cell line HUVEC decreased significantly by 37% in cell count ( $P < .001$ ); however, viability of HUVEC detected by an MTT-based assay was only marginally affected (approximately 10%) and only at the highest SLT-VEGF concentration.

**Capillary tube formation assay.** The biologic activity of SLT-VEGF was evaluated in an *in vitro* bioassay of angiogenesis. The HUVEC capillary tube formation assay on a Matrigel synthetic basement membrane is a widely used *in vitro* system to model effectively the distinct temporal and spatial events underlying angiogenesis *in vivo* [28]. SLT-VEGF

displayed statistically significant dose-related inhibition of complete HUVEC capillary tube formation. VEGF-induced capillary tube formation was inhibited by 24.3% at 1 nM and by 50.8% at 10 nM SLT-VEGF. Exogenous stimulation with VEGF significantly increased HUVEC tube formation (Figure 3).

### In Vivo

**Volumes of primary tumors.** All control animals developed extensive tumor growth (AsPC-1:  $1550 \pm 131 \text{ mm}^3$ ; HPAF-2:  $3920 \pm 184 \text{ mm}^3$ ), whereas there was significantly reduced tumor growth in the SLT-VEGF and gemcitabine monotherapy groups and in SLT-VEGF plus gemcitabine combination group. For tumors derived from poorly differentiated AsPC-1 cells, treatment with SLT-VEGF resulted in a reduced tumor volume of  $487 \pm 56 \text{ mm}^3$  (-69%) in the prophylaxis group and  $492 \pm 72 \text{ mm}^3$  (-68% reduction) in the therapy group. Treatment with gemcitabine was somewhat less effective and reduced the volume of AsPC-1 tumors to  $678 \pm 115 \text{ mm}^3$  (-56% reduction) in the prophylaxis group and to  $928 \pm 491 \text{ mm}^3$  (-40% reduction) in the therapy group. However, the combination of SLT-VEGF with gemcitabine was significantly most effective in AsPC-1 tumors than either monotherapy

and inhibited primary tumor growth to  $177 \pm 31 \text{ mm}^3$  (-89% reduction) in the prophylaxis group and to  $360 \pm 76 \text{ mm}^3$  (-77% reduction) in the therapy group (Figure 4A).

Tumors derived from the moderately differentiated HPAF-2 cells were reduced by SLT-VEGF treatment to  $1069 \pm 267 \text{ mm}^3$  (-73% reduction) in the prophylaxis group and to  $1587 \pm 167 \text{ mm}^3$  (-60% reduction) in the therapy group. Treatment with gemcitabine was significantly more effective and diminished tumor growth of the HPAF-2 tumors to  $184 \pm 133 \text{ mm}^3$  (-95% reduction) in the prophylaxis group and to  $361 \pm 284 \text{ mm}^3$  (-91% reduction) in the therapy group. Interestingly, combination of both substances did not prove to be more effective than gemcitabine alone and reduced tumor growth of HPAF-2 tumors to  $178 \pm 204 \text{ mm}^3$  (-95% reduction) in the prophylaxis group and to  $711 \pm 270 \text{ mm}^3$  (-82% reduction) in the treatment group (Figure 4A).

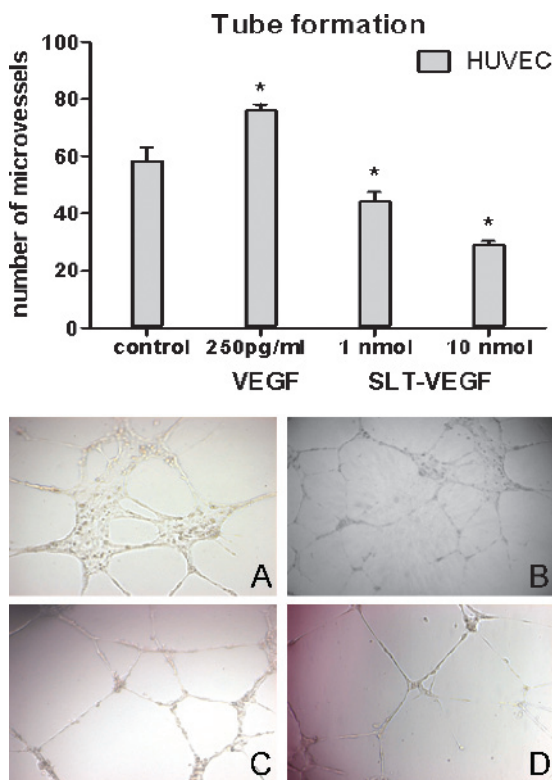
**Tumor dissemination.** Local infiltration and distant metastasis were summarized by a dissemination score. Control animals with tumors derived from the poorly differentiated AsPC-1 cell line reached a high score ( $20.4 \pm 2.5$  points). Treatment with SLT-VEGF tended to result in a reduction of tumor spread to  $13.2 \pm 2.4$  points in the prophylaxis group and was not effective ( $18.6 \pm 2.0$  points) in the therapy group. Animals treated with gemcitabine showed no difference in tumor spread in comparison to control animals ( $22.6 \pm 4.2$  points, prophylaxis group;  $23.7 \pm 9.2$  points, therapy group). Combined treatment with SLT-VEGF and gemcitabine resulted in a significant reduction of tumor dissemination in animals with AsPC-1 tumors in the prophylaxis group ( $8.0 \pm 1.1$  points) and in the therapy group ( $9.8 \pm 2.4$  points; Figure 4B).

Tumors derived from the HPAF-2 cell line also displayed a high dissemination score ( $17.0 \pm 1.2$  points). Administration of SLT-VEGF reduced tumor spread to  $10.4 \pm 2.2$  points in the prophylaxis group but not in the therapy group ( $15.9 \pm 2.7$  points). Treatment with gemcitabine inhibited tumor dissemination significantly to  $1.2 \pm 1.0$  points in the prophylaxis group and to  $3.4 \pm 1.5$  points in the therapy group. Tumor spread was almost completely suppressed after combined treatment with SLT-VEGF and gemcitabine in the prophylaxis group ( $0.58 \pm 1.2$  points) and significantly reduced in the therapy group ( $4.4 \pm 2.3$  points; Figure 4B).

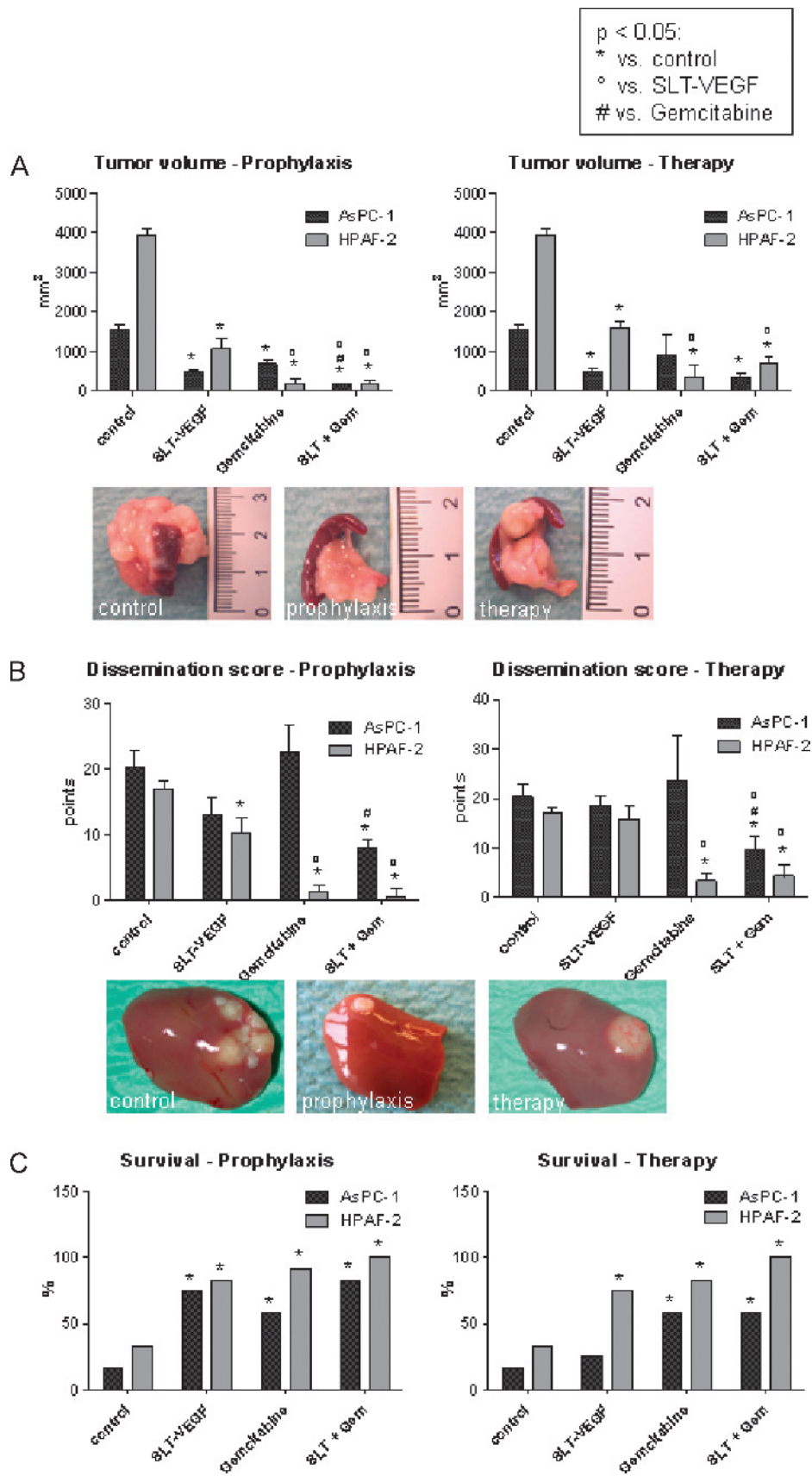
**Survival.** The AsPC-1 tumors showed a relative aggressive behavior *in vivo*, which was reflected in a low 14-week survival of the controls (17%). Monotherapy with SLT-VEGF revealed a trend to increase survival rates in the therapy group (25%) and increased 14-week survival in the prophylaxis group to 75% ( $P < .05$ ). Treatment with gemcitabine resulted in an increase of survival rates to 58% in both therapy and prophylaxis groups. Combination of SLT-VEGF with gemcitabine revealed a tendency toward increased 14-week survival in the therapy (58%) and the prophylaxis groups (83%; Figure 4C).

Tumors derived from the HPAF-2 tumors grew less aggressively than AsPC-1 tumors and resulted in higher 14-week survival (33% vs 17%). Monotherapy with SLT-VEGF increased survival to 75% in the therapy group and 83% in prophylaxis group. Gemcitabine alone led to an increased survival of 83% in the therapy group and of 92% in the prophylaxis group. The combined treatment of SLT-VEGF and gemcitabine resulted in a 100% survival in both (therapy and prophylaxis) groups (Figure 4C).

**Microvessel density.** As a parameter of angiogenic activity, MVD was determined by immunohistochemistry using anti-CD31 as an endothelial marker. MVD was enhanced 4.6- and 5.3-fold in the



**Figure 3.** Dose-related effect of SLT-VEGF on capillary tube formation of HUVEC after 18 hours of incubation on Matrigel basement membrane; stimulation with VEGF served as positive control. Complete capillary tube networks within a designated area were counted under light microscopy (magnification,  $\times 10$ ), and the data were expressed as percentage inhibition of complete capillary tube formation relative to untreated HUVEC control cultures incubated under the same conditions. Photomicrographs ( $\times 100$ ) of HUVEC capillary tube formation in untreated cultures (A), 250 pg/ml VEGF (B), 1 nM SLT-VEGF (C), and 10 nM SLT-VEGF (D); \* $P < .05$  versus control, respectively.



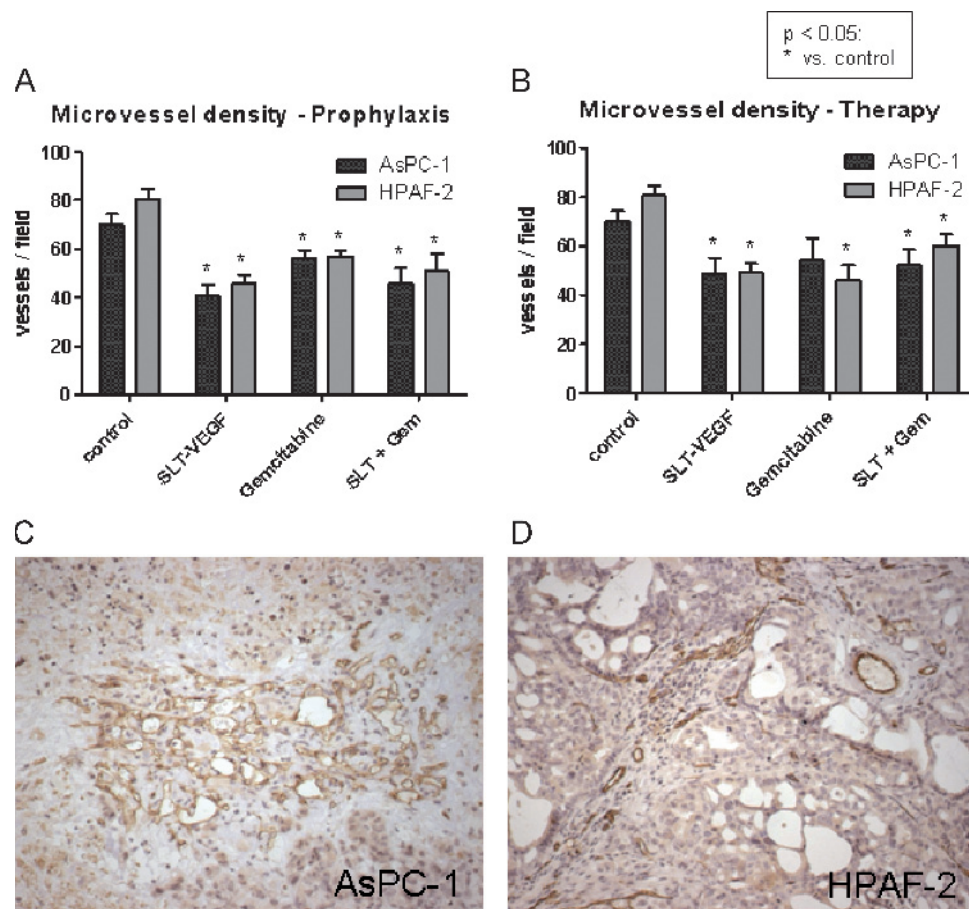


**Figure 5.** MVD in primary tumors of controls and animals treated with SLT-VEGF, gemcitabine, or the combination therapy was determined by immunohistochemistry for CD31 (A, prophylactic treatment; B, therapeutic treatment). Primary tumors were derived from the cell lines AsPC-1 (C, control animal; magnification,  $\times 200$ ) and HPAF-2 (D, control animal; magnification,  $\times 200$ ).

untreated AsPC-1 and HPAF-2 primary tumors, respectively, compared with normal exocrine pancreas (AsPC-1,  $70.0 \pm 4.3/0.74 \text{ mm}^2$ ; HPAF-2,  $80.5 \pm 4.3/0.74 \text{ mm}^2$ ; native pancreas,  $15.6 \pm 1.5/0.74 \text{ mm}^2$ ;  $P < .001$ ).

Treatment with SLT-VEGF significantly reduced MVD of AsPC-1 primary tumors in the prophylaxis group ( $40.8 \pm 4.3/0.74 \text{ mm}^2$ ) and in the therapy group ( $48.9 \pm 6.1/0.74 \text{ mm}^2$ ). Administration of gemcitabine resulted in a reduced MVD in animals of the prophylaxis group ( $56.1 \pm 3.3/0.74 \text{ mm}^2$ ) as well as in the therapy group ( $54.0 \pm 18.7/0.74 \text{ mm}^2$ ). Combined treatment with SLT-VEGF and gemcitabine showed no additional benefit in reducing MVD ( $46.0 \pm 6.1/0.74 \text{ mm}^2$  prophylaxis group;  $52.2 \pm 6.3/0.74 \text{ mm}^2$  therapy group; Figure 5, A-C).

In animals with HPAF-2 tumors, treatment with SLT-VEGF resulted in a significant reduction of MVD in both groups ( $45.9 \pm 3.5/0.74 \text{ mm}^2$ , prophylaxis;  $49.3 \pm 3.5/0.74 \text{ mm}^2$ , therapy). Monotherapy with gemci-

tabine reduced MVD in the prophylaxis group ( $57.0 \pm 2.4/0.74 \text{ mm}^2$ ) and the therapy group ( $46.3 \pm 11.7/0.74 \text{ mm}^2$ ). Combination of SLT-VEGF and gemcitabine resulted in no further reduction of MVD in the prophylaxis group ( $50.8 \pm 14.3/0.74 \text{ mm}^2$ ) and in the therapy group ( $60.3 \pm 4.6/0.74 \text{ mm}^2$ ; Figure 5, A, B, and D).

**Immunohistochemical analysis of VEGF and its receptors.** To determine the immunohistochemical localization of VEGF and its receptors Flt1/VEGFR-1 and KDR/FLK1/VEGFR-2, highly specific polyclonal antibodies were used. Moderate to strong VEGF immunoreactivity was found in the cytoplasm of pancreatic cancer cells of AsPC-1 and HPAF-2 tumors (Figure 6, A and B). Both cell lines were also mildly to moderately immunoreactive for VEGFR-1 but not for VEGFR-2 (Figure 6, C-F). VEGFR-2 was only detected in endothelial cells of the tumors (Figure 6, G and H).

**Figure 4.** Orthotopic pancreatic cancer was derived from poorly differentiated AsPC-1 and moderately differentiated HPAF-2 cells. Treatment started after either 3 days (prophylaxis) or 6 weeks (therapy) and was continued up to 14 weeks. (A) Volume of the primary tumor in control mice and animals treated with SLT-VEGF, gemcitabine, or the combination therapy. Images are representative of primary tumors derived from AsPC-1 cancer cells (control, after prophylactic SLT-VEGF treatment, after therapeutic SLT-VEGF treatment). (B) Dissemination scores, quantifying local and distant tumor spread, in control mice and animals treated with SLT-VEGF, gemcitabine, or the combination therapy. Images are representative for liver metastasis; primary tumors were derived from AsPC-1 cancer cells (control, after prophylactic SLT-VEGF treatment, after therapeutic SLT-VEGF treatment). (C) Fourteen-week survival in control mice and animals treated with SLT-VEGF, gemcitabine, or the combination therapy.

## Discussion

Targeting proangiogenic mediators such as VEGF and VEGFR-2 has emerged as a promising anticancer treatment strategy, especially for devastating malignancies such as exocrine pancreatic cancer, which is virtually incurable by surgical resection and/or chemoradiation [29,30]. Growth of primary tumor and metastatic lesions beyond the size of a few cubic millimeters requires neovascularization that combines angiogenesis and vasculogenesis. Therefore, inhibition of angiogenesis is an attractive and promising target for tumor therapy because it theoretically offers the hope of long-term control of neoplasm progression [3]. Kuehn et al. [8] demonstrated that MVD and expression of proangiogenic factors such as VEGF were significantly higher in pancreatic cancer in comparison to the normal pancreas. The VEGF receptors are expressed at high levels in the activated endothelium of tumor vasculature in general [31] and in pancreatic cancer, specifically [32], whereas normal mature blood vessels show

negligible levels of VEGF receptors [33]. Our previous research demonstrated that systemic treatment with VEGF coupled to diphtheria-toxin (DT-VEGF) led to specific targeting and damaging of tumor blood vessels [34].

In this study, we investigated a more specific approach: the effect of the immunotoxin SLT-VEGF that selectively targets endothelial cells overexpressing VEGFR-2 [17,18,22]. Using two cancer animal models, syngeneic 4T1 murine breast cancer and PC3 human prostate cancer xenografts, we have previously demonstrated that three to five biweekly injections of SLT-VEGF fusion protein inhibited tumor growth approximately two-fold [18]. Detailed immunohistochemical analysis of 4T1 tumors revealed that SLT-VEGF treatment only mildly (1- to 1.4-fold) decreases the overall prevalence of CD31<sup>+</sup> tumor endothelial cells. In contrast, the prevalence of VEGFR-2-overexpressing tumor endothelial cells decreased four- to five-fold [19]. These findings were supported by the results of whole body imaging

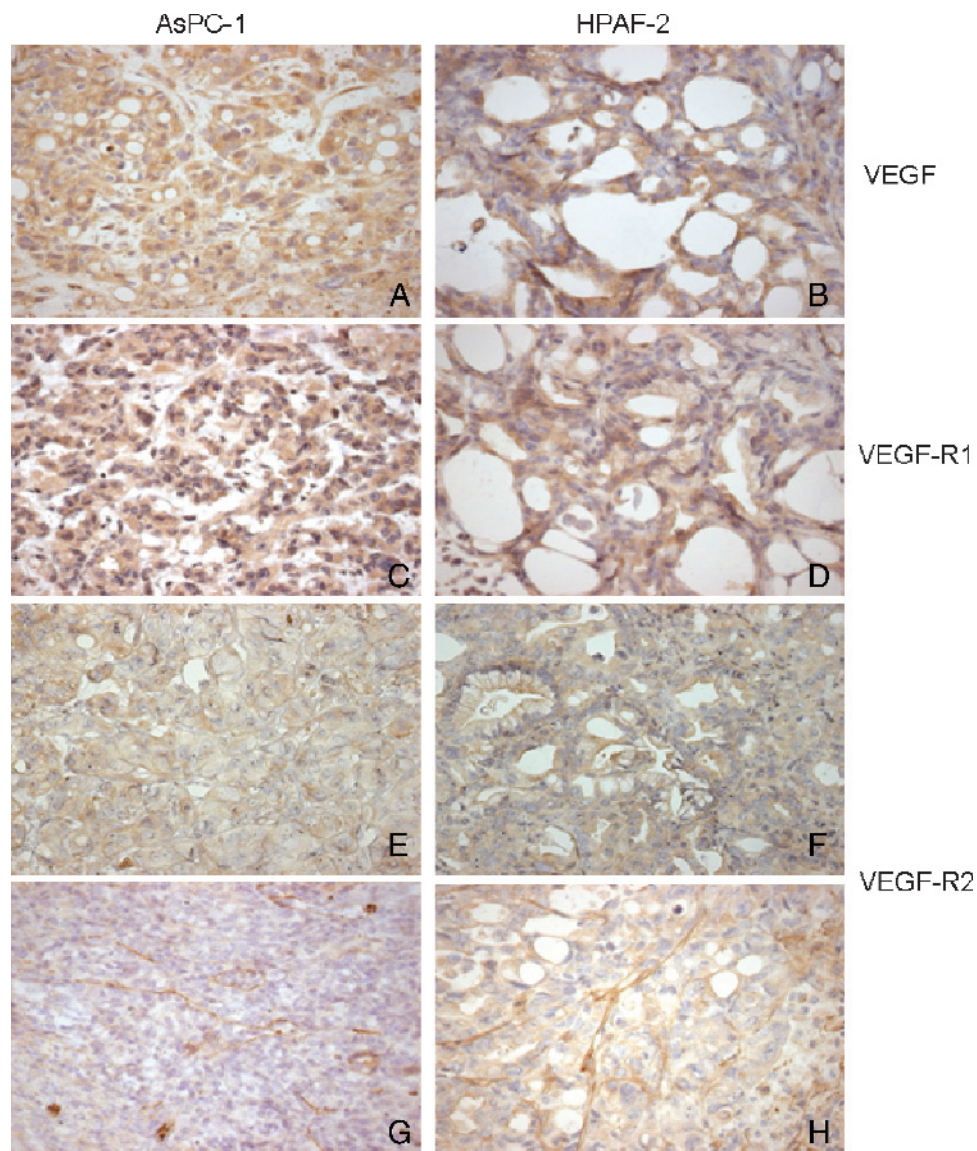


**Figure 6.** Immunostaining (brown color) of orthotopic tumors in nude mice derived from the human pancreatic cancer cell lines AsPC-1 and HPAF-2 revealed expression of VEGF (A, B) and Flt/VEGFR-1 (C, D) in tumor cells, thereby confirming RT-PCR results (Figure 1). Pancreatic cancer cells were negative for KDR/FLK1/VEGFR-2 (E, F) in contrast to VEGFR-2-positive endothelial cells (G, H). Magnification,  $\times 200$ .



of VEGFR-2 in tumor vasculature with VEGF-based near-infrared fluorescent tracers [22]. In these experiments, SLT-VEGF treatment dramatically inhibited VEGFR-2-mediated accumulation of tracers in tumor endothelial cells, reflecting the depletion of endothelial cells overexpressing VEGFR-2 [22]. Taken together, *in vitro* and *in vivo* results indicate that SLT-VEGF may be less toxic for normal endothelial cells of the host organism but targets predominantly proliferating tumor endothelial cells with reportedly upregulated expression of VEGFR-2 [11]. Using two cancer animal models, syngeneic 4T1 murine breast cancer and PC3 human prostate cancer xenografts, we have previously demonstrated that SLT-VEGF fusion protein inhibited tumor growth by selective elimination of tumor endothelial cells expressing high levels of VEGFR-2 [22]. This indicates that SLT-VEGF may be less toxic for normal endothelial cells of the host organism but targets predominantly proliferating tumor endothelial cells with reportedly upregulated expression of VEGFR-2 [11]. Indeed, as we report here human endothelial cell line HUVEC, a model system for normal endothelial cells with physiological level of VEGFR-2 expression showed a somewhat decreased proliferation (Figure 2A) and tube formation (Figure 3) but not viability (Figure 2B). In contrast, DT-VEGF was reported to be cytotoxic to HUVECs [35].

The antitumor effects of SLT-VEGF were evaluated in an orthotopic nude mouse model of pancreatic cancer, which was established in our laboratory [24]. This model mirrors the development of this clinical disease and allows assessment not only of primary tumor growth but also of metastasis and survival. Importantly, both pancreatic cancer cell lines AsPC-1 and HPAF-2 used in these models were not sensitive to SLT-VEGF (Figure 2), indicating that its therapeutic effects are due predominantly to the sensitivity of endothelial cells. Furthermore, in both models, selected regimens of SLT-VEGF (200  $\mu\text{g}/\text{kg}$ , gemcitabine, or both drugs) did not exhibit any clinical evidence of toxicity, such as a change in food intake or activity in treatment groups, compared with control animals.

Poorly differentiated AsPC-1 tumors displayed an aggressive growth pattern, killing most control animals before the end of the 14-week observation period. SLT-VEGF treatment, started either 3 days (prophylaxis group) or 6 weeks (treatment group) after tumor implantation, reduced microvascular density in primary tumors 1.7- and 1.4-fold, respectively. Remarkably, these rather modest changes in microvascular density were associated with reduced primary tumor volume (up to -69%), increased survival (up to +58%; Figure 4, A and C), and decreased tumor dissemination in the prophylaxis group (Figure 4B).

Moderately differentiated HPAF-2 cells grew to large, partly cystic tumors in control mice and displayed a moderate local and systemic pattern of spread. The response to SLT-VEGF treatment was similar to that observed in poorly differentiated AsPC-1 tumors: moderate decrease in microvascular density (Figure 5, A and B), rather dramatic decrease in tumor volume and increase in survival, and inhibition of tumor dissemination in the prophylaxis group (Figure 4B).

It is interesting to compare the effects of SLT-VEGF with those of gemcitabine, the frontline drug for advanced pancreatic cancer. Gemcitabine monotherapy resulted in an increased survival (AsPC-1, up to 58%; HPAF-2, up to 92%; Figure 4C), and a decreased primary tumor volume (Figure 4A). Tumor dissemination of AsPC-1 tumors was almost unaffected in gemcitabine treatment group (Figure 4B). It seems that SLT-VEGF is somewhat more effective in inhibiting tumor growth and metastatic dissemination, as well as overall survival, in the poorly differentiated AsPC-1 model. In contrast, gemcitabine was more effective in inhibiting tumor growth and metastatic dissemination in the

moderately differentiated HPAF-2 model. Importantly, in both models, combination of both drugs provided for a tendency toward better survival, lower primary tumor volume, and reduced tumor dissemination, especially in the prophylaxis groups of both AsPC-1 and HPAF-2 tumors (Figure 4, A-C). However, this tendency did not reach statistical significance for all parameters. It may be due to the significant antitumor effects of the respective monotherapies at tested regimens, especially in the HPAF-2 group, which were difficult to improve by the combination. In turn, it suggests that there might be opportunities for decreasing doses of each component without losing therapeutic benefits of the combination. Furthermore, these results suggest that combination of SLT-VEGF and gemcitabine might require careful optimization to reach the most advantageous synergy. For example, because SLT-VEGF is more cytotoxic to cells overexpressing VEGFR-2, treatment with this cytotoxin might be more effective if timed to the stages when tumor vasculature is enriched with such cells, for example, in response to treatment with other drugs.

Interestingly, SLT-VEGF and gemcitabine induced rather similar decreases in microvascular density in both tumor models. SLT-VEGF targets tumor endothelial cells overexpressing VEGFR-2, selectively depleting tumor vasculature of such cells [19]. However, gemcitabine, a fluorinated analog of deoxycytidine, is toxic to proliferating endothelial cells because it inhibits DNA replication either directly or indirectly through inactivation of the RNA reductase. Thus, if actively growing tumor endothelial cells overexpress VEGFR-2, they would be targets for both SLT-VEGF and gemcitabine, and both drugs might lead to similar decreases in microvascular density.

In summary, this study adds further evidence that angiogenesis is a critical component of pancreatic cancer growth and metastasis. Currently, there are multiple clinical trials in progress for combination of antiangiogenic drugs, such as bevacizumab, sunitinib, or sorafenib, with chemotherapeutic agents, such as gemcitabine ([www.cilicaltrials.gov](http://www.cilicaltrials.gov)). Although there is no definitive model for combination of antiangiogenic and chemotherapeutic drugs, there are suggestions that delivery of chemotherapeutics to tumor cells might be more efficient when provided by tumor vasculature responding to antiangiogenic treatment. It remains to be established whether such improved delivery takes place and whether it is associated with "normalization" of tumor vasculature [36] or with continuous revascularization of tumors in response to drugs, particularly those delivered through metronomic scheduling [37]. However, regardless of mechanism, it seems that pancreatic cancers are sensitive to combinations of chemotherapeutic and antiangiogenic drugs. In this respect, our finding that targeting VEGFR-2-overexpressing tumor endothelial cells with SLT-VEGF fusion protein resulted in a significant biologic improvement in two clinically relevant orthotopic pancreatic tumor models, comparable to that induced by gemcitabine, seems particularly significant. We believe that optimization of the SLT-VEGF/gemcitabine regimen provides a promising treatment strategy for advanced pancreatic cancer.

## References

- [1] Jemal A, Siegel R, Ward E, Hao Y, Xu J, and Thun MJ (2009). Cancer statistics, 2009. *CA Cancer J Clin* **59**, 225-249.
- [2] Folkman J (1995). Angiogenesis in cancer, vascular, rheumatoid and other disease. *Nat Med* **1**, 27-31.
- [3] Brown JM and Giaccia AJ (1998). The unique physiology of solid tumors: opportunities (and problems) for cancer therapy. *Cancer Res* **58**, 1408-1416.
- [4] Neufeld G, Cohen T, Gengrinovitch S, and Poltorak Z (1999). Vascular endothelial growth factor (VEGF) and its receptors. *FASEB J* **13**, 9-22.

- [5] Veikkola T, Karkkainen M, Claesson-Welsh L, and Alitalo K (2000). Regulation of angiogenesis via vascular endothelial growth factor receptors. *Cancer Res* **60**, 203–212.
- [6] Itakura J, Ishiwata T, Friess H, Fujii H, Matsumoto Y, Buchler MW, and Korc M (1997). Enhanced expression of vascular endothelial growth factor in human pancreatic cancer correlates with local disease progression. *Clin Cancer Res* **3**, 1309–1316.
- [7] Itakura J, Ishiwata T, Shen B, Kornmann M, and Korc M (2000). Concomitant over-expression of vascular endothelial growth factor and its receptors in pancreatic cancer. *Int J Cancer* **85**, 27–34.
- [8] Kuehn R, Lelkes PI, Bloechle C, Niendorf A, and Izbicki JR (1999). Angiogenesis, angiogenic growth factors, and cell adhesion molecules are upregulated in chronic pancreatic diseases: angiogenesis in chronic pancreatitis and in pancreatic cancer. *Pancreas* **18**, 96–103.
- [9] Seo Y, Baba H, Fukuda T, Takashima M, and Sugimachi K (2000). High expression of vascular endothelial growth factor is associated with liver metastasis and a poor prognosis for patients with ductal pancreatic adenocarcinoma. *Cancer* **88**, 2239–2245.
- [10] Ikeda N, Adachi M, Taki T, Huang C, Hashida H, Takabayashi A, Sho M, Nakajima Y, Kanehiro H, Hisanaga M, et al. (1999). Prognostic significance of angiogenesis in human pancreatic cancer. *Br J Cancer* **79**, 1553–1563.
- [11] Brown LF, Berse B, Jackman RW, Tognazzi K, Manseau EJ, Dvorak HF, and Senger DR (1993). Increased expression of vascular permeability factor (vascular endothelial growth factor) and its receptors in kidney and bladder carcinomas. *Am J Pathol* **143**, 1255–1262.
- [12] Drevs J, Hofmann I, Hugenschmidt H, Wittig C, Madjar H, Muller M, Wood J, Martiny-Baron G, Unger C, and Marme D (2000). Effects of PTK787/ZK 222584, a specific inhibitor of vascular endothelial growth factor receptor tyrosine kinases, on primary tumor, metastasis, vessel density, and blood flow in a murine renal cell carcinoma model. *Cancer Res* **60**, 4819–4824.
- [13] Wedge SR, Ogilvie DJ, Dukes M, Kendrew J, Curwen JO, Hennequin LF, Thomas AP, Stokes ES, Curry B, Richmond GH, et al. (2000). ZD4190: an orally active inhibitor of vascular endothelial growth factor signaling with broad-spectrum antitumor efficacy. *Cancer Res* **60**, 970–975.
- [14] Wedge SR, Kendrew J, Hennequin LF, Valentine PJ, Barry ST, Brave SR, Smith NR, James NH, Dukes M, Curwen JO, et al. (2005). AZD2171: a highly potent, orally bioavailable, vascular endothelial growth factor receptor-2 tyrosine kinase inhibitor for the treatment of cancer. *Cancer Res* **65**, 4389–4400.
- [15] Brekken RA, Overholser JP, Stastny VA, Waltenberger J, Minna JD, and Thorpe PE (2000). Selective inhibition of vascular endothelial growth factor (VEGF) receptor 2 (KDR/Flk-1) activity by a monoclonal anti-VEGF antibody blocks tumor growth in mice. *Cancer Res* **60**, 5117–5124.
- [16] Vitaliti A, Wittmer M, Steiner R, Wyder L, Neri D, and Klemenz R (2000). Inhibition of tumor angiogenesis by a single-chain antibody directed against vascular endothelial growth factor. *Cancer Res* **60**, 4311–4314.
- [17] Bergers G and Hanahan D (2008). Modes of resistance to anti-angiogenic therapy. *Nat Rev Cancer* **8**, 592–603.
- [18] Backer MV and Backer JM (2001). Targeting endothelial cells overexpressing VEGFR-2: selective toxicity of Shiga-like toxin-VEGF fusion proteins. *Bioconjug Chem* **12**, 1066–1073.
- [19] Backer MV, Hamby CV, and Backer JM (2009). Inhibition of vascular endothelial growth factor receptor signaling in angiogenic tumor vasculature. *Adv Genet* **67**, 1–27.
- [20] Obrigg TG, Del Vecchio PJ, Karmali MA, Petric M, Moran TP, and Judge TK (1987). Pathogenesis of haemolytic uraemic syndrome. *Lancet* **2**, 687.
- [21] Obrigg TG, Louise CB, Lingwood CA, Boyd B, Barley-Maloney L, and Daniel TO (1993). Endothelial heterogeneity in Shiga toxin receptors and responses. *J Biol Chem* **268**, 15484–15488.
- [22] Backer MV, Gaynutdinov TI, Patel V, Bandyopadhyaya AK, Thirumamagal BTS, Tjarks W, Barth R, Claffey KP, and Backer JM (2005). Vascular endothelial growth factor selectively targets boronated dendrimers to tumor vasculature. *Mol Cancer Ther* **4**, 1423–1429.
- [23] Gitay-Goren H, Cohen T, Tessler S, Soker S, Gengrinovitch S, Rockwell P, Klagsbrun M, Levi BZ, and Neufeld G (1996). Selective binding of VEGF<sub>121</sub> to one of the three vascular endothelial growth factor receptors of vascular endothelial cells. *J Biol Chem* **271**, 5519–5523.
- [24] Hotz HG, Reber HA, Hotz B, Yu T, Foitzik T, Buhr HJ, Cortina G, and Hines OJ (2003). An orthotopic nude mouse model for evaluating pathophysiology and therapy of pancreatic cancer. *Pancreas* **26**, e89–e98.
- [25] Hotz HG, Reber HA, Hotz B, Foitzik T, Buhr HJ, Cortina G, and Hines OJ (2001). An improved clinical model of orthotopic pancreatic cancer in immunocompetent Lewis rats. *Pancreas* **22**, 113–121.
- [26] Weidner N (1998). Tumour vascularity as a prognostic factor in cancer patients: the evidence continues to grow [comment]. *J Pathol* **184**, 119–122.
- [27] Veenendaal LM, Jin H, Ran S, Cheung L, Navone N, Marks JW, Waltenberger J, Thorpe P, and Rosenblum MG (2002). *In vitro* and *in vivo* studies of a VEGF<sub>121</sub>/rGelonin chimeric fusion toxin targeting the neovasculature of solid tumors. *Proc Natl Acad Sci USA* **99**, 7866–7871.
- [28] Vailhe B, Vittet D, and Feige JJ (2001). *In vitro* models of vasculogenesis and angiogenesis. *Lab Invest* **81**, 439–452.
- [29] Philip PA (2008). Targeted therapies for pancreatic cancer. *Gastrointest Cancer Res* **2**, S16–S19.
- [30] Philip PA (2008). Targeting angiogenesis in pancreatic cancer. *Lancet* **371**, 2062–2064.
- [31] Zhang Z, Neiva KG, Lingen MW, Ellis LM, and Nor JE (2009). VEGF-dependent tumor angiogenesis requires inverse and reciprocal regulation of VEGFR1 and VEGFR2. *Cell Death Differ*.
- [32] von Marschall Z, Cramer T, Hocker M, Burde R, Plath T, Schirner M, Heidenreich R, Breier G, Riecken EO, Wiedenmann B, et al. (2000). *De novo* expression of vascular endothelial growth factor in human pancreatic cancer: evidence for an autocrine mitogenic loop. *Gastroenterology* **119**, 1358–1372.
- [33] Wild R, Dhanabal M, Olson TA, and Ramakrishnan S (2000). Inhibition of angiogenesis and tumour growth by VEGF<sub>121</sub>-toxin conjugate: differential effect on proliferating endothelial cells. *Br J Cancer* **83**, 1077–1083.
- [34] Hotz HG, Gill PS, Masood R, Hotz B, Buhr HJ, Foitzik T, Hines OJ, and Reber HA (2002). Specific targeting of tumor vasculature by diphtheria toxin-vascular endothelial growth factor fusion protein reduces angiogenesis and growth of pancreatic cancer. *J Gastrointest Surg* **6**, 159–166, discussion 166.
- [35] Ramakrishnan S, Olson TA, Bautch VL, and Mohanraj D (1996). Vascular endothelial growth factor-toxin conjugate specifically inhibits KDR/flk-1-positive endothelial cell proliferation *in vitro* and angiogenesis *in vivo*. *Cancer Res* **56**, 1324–1330.
- [36] Jain RK (2005). Normalization of tumor vasculature: an emerging concept in antiangiogenic therapy. *Science* **307**, 58–62.
- [37] Kerbel RS and Kamen BA (2004). The anti-angiogenic basis of metronomic chemotherapy. *Nat Rev Cancer* **4**, 423–436.

## Supplementary Material

### Stability of SLT-VEGF

SLT-VEGF stability in PBS and murine serum was assessed after 2 hours of incubation at 37°C. Western blot analysis was used to assess physical integrity, and cytotoxicity assay was used to assess functional activity.

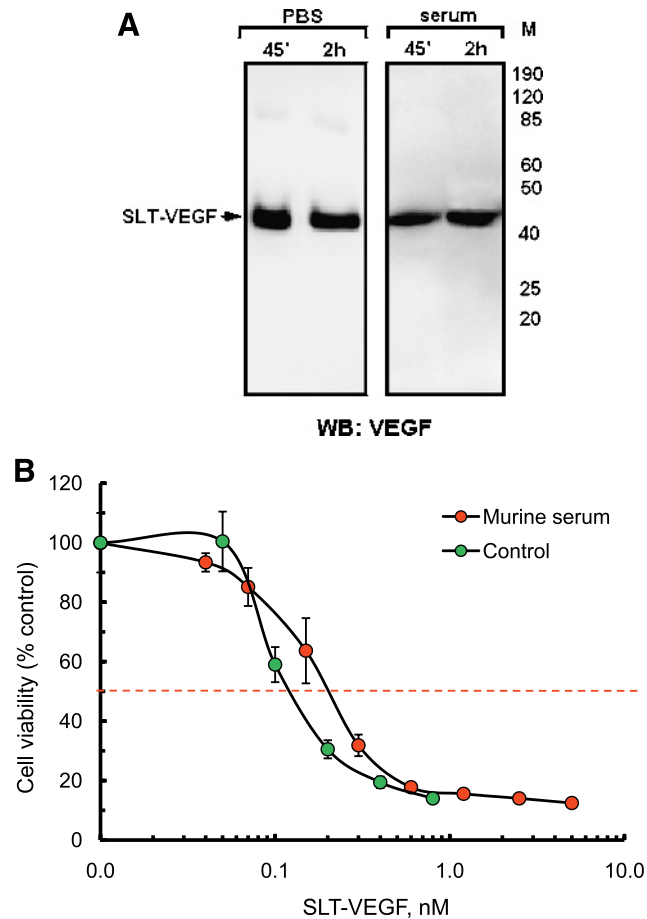


**Figure W1.** (A) SLT-VEGF remains stable in PBS and serum after a 2-hour incubation at 37°C. Murine serum was collected as described [19] and stored frozen at  $-20^{\circ}\text{C}$  in small aliquots until needed. SLT-VEGF was added to murine serum (or PBS) to a final concentration of  $1\ \mu\text{M}$  and incubated at  $37^{\circ}\text{C}$ . Protein samples collected after 45 minutes and 2 hours of incubation were separated by reducing 12.5% SDS-PAGE gel and analyzed by Western blot analysis using a rabbit VEGF-specific antibody A-20 (Santa Cruz Biotechnology) followed by antirabbit-HRP conjugate (GE Healthcare, Waukesha, WI). M indicates molecular weight markers. (B) SLT-VEGF retains cytotoxic activity after a 2-hour incubation at  $37^{\circ}\text{C}$  in murine serum. The cytotoxicity assay is described in Backer et al. [18]. Briefly, 293/KDR cells (SibTech, Inc, Brookfield, CT) expressing  $2 \times 10^6$  VEGFR-2 per cell were seeded onto 96-well plates at a density of  $2 \times 10^3$  cells per well, in 0.05 ml of Dulbecco's modified Eagle medium complete per well. Twenty hours later, SLT-VEGF incubated in complete murine serum for 2 hours at  $37^{\circ}\text{C}$ , or freshly thawed control SLT-VEGF, were serially diluted in Dulbecco's modified Eagle medium complete and added to cells in triplicate wells, 0.05 ml/well, to make the final volume of 0.1 ml per well at the indicated SLT-VEGF concentrations. After 96 hours of incubation under normal culture conditions, viable cells were determined by CellTiter 96 AQ<sub>UEOUS</sub> One Solution Cell Proliferation Assay kit (Promega, Madison, WI). The assay was done in triplicate.

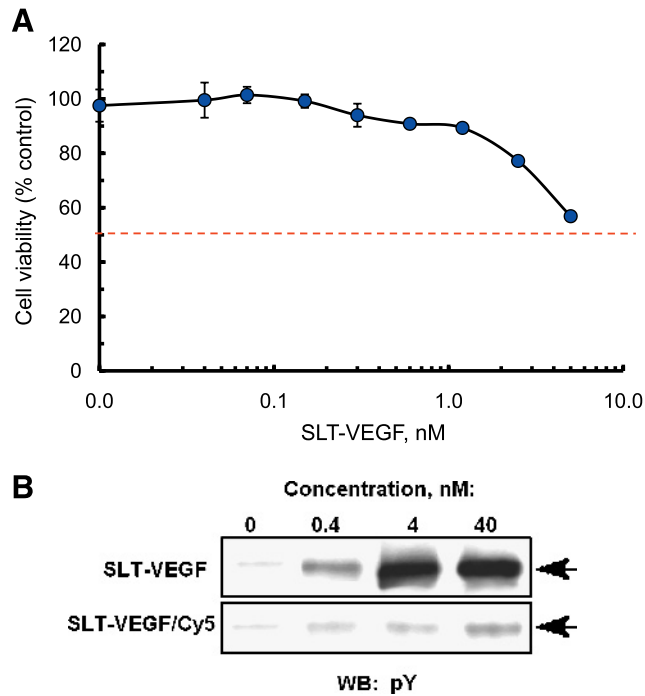


**Figure W2.** Direct modification with a fluorescent dye dramatically reduces the functional activity of SLT-VEGF. Preparation of SLT-VEGF/Cy5 conjugate. In a series of pilot experiments, we optimized conditions of modification to obtain fluorescent SLT-VEGF with no more than one molecule of Cy5 dye per SLT-VEGF. The selected conditions were as follows: 43 nmol of SLT-VEGF was mixed with Cy5-NHS (GE Healthcare) in 0.1 M NaPi buffer of pH 7.2, to a final molar ratio of four NHS groups per one SLT-VEGF protein. After 1 hour of incubation at room temperature, unreacted NHS was quenched by addition of 1:10 vol./vol. part of 1 M Tris-HCl pH 8.0 and incubation for 30 minutes at room temperature. Modified protein was purified by a combination of ion exchange chromatography on Q-Sepharose FF (1-ml prepacked columns; GE Healthcare) and gel filtration (PD-10 columns; GE Healthcare). Purified SLT-VEGF/Cy5 was analyzed reverse phase high-performance liquid chromatography profile on C4 Alltech Macro-sphere column (Alltech, Iselin, NJ). The extent of SLT-VEGF modification was determined by analysis of peak intensities at 216 nm, for protein, and 598 nm, for Cy5 (Backer 2007). RP HPLC analysis revealed that purified SLT-VEGF/Cy5 contained one molecule of Cy5 dye per protein. Two assays, cytotoxicity and induction of VEGFR-2 tyrosine phosphorylation, were used to assess the functional activity of SLT-VEGF/Cy5. In both assays, SLT-VEGF/Cy5 was dramatically less active than parental SLT-VEGF, indicating that conjugating even a single Cy5 per SLT-VEGF dramatically decreases the ability of protein to bind to VEGFR-2 and become internalized via VEGFR-2-mediated endocytosis. (A) Cytotoxicity of SLT-VEGF/Cy5 is dramatically decreased. The cytotoxicity of SLT-VEGF/Cy5 was tested using 293/KDR cells, as described [18] (see also Figure W1B). In this assay, 50% inhibition of cell growth was not reached at 5 nM SLT-VEGF/Cy5, as opposed to the  $IC_{50}$  value of 0.1 nM for parental SLT-VEGF (Figure W1A). (B) The ability of SLT-VEGF/Cy5 to activate VEGFR-2 is dramatically reduced. The reduced cytotoxicity of SLT-VEGF/Cy5 might be a result of either damaged enzymatic activity of the SLT moiety or the reduced ability of the VEGF moiety to bind to VEGFR-2 and deliver the fusion protein inside the cell through receptor-mediated internalization. To assess the ability of SLT-VEGF/Cy5 to bind to and activate VEGFR-2, we used induction of VEGFR-2 tyrosine phosphorylation in 293/KDR cells assay (as described in Backer and Backer [18]). Briefly, near-confluent 293/KDR cells after overnight starvation were stimulated with varying amounts of SLT-VEGF or fluorescent SLT-VEGF/Cy5, for 10 minutes at 37°C and then lysed and analyzed by Western blot analysis using anti-phosphotyrosine antibody PT-66 (Sigma, St Louis, MO). Arrows indicate the position of VEGFR-2. pY indicates phosphotyrosine. Note that VEGFR-2 tyrosine phosphorylation is dramatically lower on stimulation with SLT-VEGF/Cy5, as opposed to parental SLT-VEGF protein. These results indicate that conjugation of a single Cy5 dye to SLT-VEGF resulted in modification of lysine residues of VEGF moiety that are critically involved in the interaction of VEGF moiety with its receptor, VEGFR-2.